Proceedings of the Sixth International Conference on
Asian and Pacific Coasts (APAC 2011)

December 14 – 16, 2011, Hong Kong, China

APPLICATION OF ROMS FOR SIMULATING EVOLUTION AND MIGRATION OF TIDAL SAND WAVES

Z.P. ZANG[1], L. CHENG[2], F.P. GAO[1]

[1]*Key Laboratory for Hydrodynamics and Ocean Engineering, Institute of Mechanics, Chinese Academy of Sciences, 15 North 4th Ring West Rd, Beijing, 100190, China*

[2]*School o f Civil and Resource Engineering, The University of Western Australia, 35 Striling HWY, Crawley, WA, 6009, Australia*

A three-dimensional morphodynamic numerical sand wave model is established based on an existing model, the Regional Oceanographic Modelling System (ROMS). In the model, the vertical flow structure, which plays an important role in the formation and evolution of sand waves, is resolved by solving three dimensional (3D) Reynolds-averaged Navier-Stokes (RANS) equations with a k-ε turbulence closure. The bed slope effect on the bedload transport is considered in the model. The model is capable of capturing sand wave evolution and migration processes, which can not be modeled by conventional stability models. First, a sensitivity analysis of the model configuration is conducted, including the morphological factor, the time step and the grid size, to find out an optimal balance between the computational time and the accuracy of results. The effects of the water depth, flow velocity and sand grain size on the Fastest Growing Mode (FGM) are then studied. Finally，a migrating artificial sand wave is simulated and numerical results are presented.

1. Introduction

Sand waves are large bed features that are often found in coastal and offshore waters. Sand waves are normally formed in the seas where the strong tide currents dominate and can be dynamic. The crests of sand waves are usually perpendicular to the direction of the mean tidal currents. Existence of sand waves will affect on-bottom stability of subsea structures.

The models developed so far in simulating the behaviors of sand waves are generally divided into two categories: stability model and numerical morphodynamic model. The stability models are mainly aimed at the long-term behavior of the sand waves with the idealized sinusoidal wave shapes and relatively small wave height. It can not simulate the transient behavior of the sand waves [1~3]. A numerical morphodynamic model can overcome the limitations of the stability model. Till now, only few numerical morphodynamic sand wave models have been reported [4,5].

It is commonly recognized that the vertical residual circulation cells induced by the interaction between the tidal flow and the perturbations in the seabed are the main cause of the generation of sand waves. Therefore accurate predictions of the vertical turbulence flow are of vital importance in simulating sand waves. Up to date most of the existing stability and numerical models employ constant viscosity turbulence models. Komarova and Hulscher (2000) had recognized the drawbacks of applying a constant eddy viscosity and improved it with a simple function of the water depth and flow velocity [2].

Most of the existing stability and numerical models impose a partial slip bottom boundary condition in calculating seabed shear stresses. This is because a partial slip bottom boundary condition can somehow compensate for errors induced by using a constant eddy viscosity. The bottom resistance is often represented by a constant resistance parameter in those models. The influences of the grain size, porosity and bottom roughness, etc, can not be reflected directly in the sediment transport calculations of these models.

So in this work, a three-dimensional numerical morphodynamic sand wave model is established based on an open-resourced model ROMS. This model has a few advantages over the previous sand wave models. The water flow is simulated by solving the 3D RANS with an accurate turbulence closure, in which the flow eddy viscosity is computed implicitly based on the local condition. The bottom shear stress can be calculated employing a validated bottom boundary layer model. The transient behaviors of the sand wave can be captured. First, the model governing equations and the numerical method are introduced briefly. Then the sensitivities of model configurations are examined. The effects of some key parameters on the Fastest Growing Mode of sand waves are studied. Finally, the model is configured to simulate an artificial sand wave under a tidal current.

2. Sand Wave Model

A 3D morphodynamic sand wave model is established based on the Regional Oceanographic Modelling System (ROMS), which is a free open-source oceanographic model developed by the United States Geological Survey (USGS) to simulate the circulation, sediment transport and the morphodynamics in coastal oceans. The water motion is solved by a set of three-dimensional Reynolds-averaged Navier-Stokes (RANS) equations with the hydrostatic and Boussinesq assumptions. The eddy viscosities and eddy diffusivities are calculated with a k-ε turbulence model in the present configuration. The governing equations are discretized by the finite-difference method in a horizontal curvilinear and vertical stretched coordinate system which makes it easy to follow the flexuous coastline and the changeful sea bottom and the freesurface. Both bedload and suspended sediment transport are considered. The details of the governing equations of the model can be found in Warner et al [6].

The effect of the bed slope on bedlod transport is considered in calculating equilibrium sand wave profile. The Meyer-Peter-Muller bed load transport formula is used to calculate the non-dimensional transport rate. Then, the volumetric sediment transport can be expressed as

$$q_{bl} = \alpha\sqrt{\left|\tau_b\right|}\left(\tau_b - \lambda_1 \frac{\partial h}{\partial x} - \lambda_2\left|\tau_b\right|\frac{\partial h}{\partial x}\right) \tag{1}$$

where, q_{bl} is the volumetric sediment transport; τ_{b} is the bed shear stress; h is the bed elevation. The calculations of coefficient α, λ_1, λ_2 are the same as those in [2]. In Eq. (1), the second term in the bracket represents the effect of bed slope on the critical Shields parameter and the third term models the effect of bed slope directly on the sediment transport.

3. Tidal-Averaged Flow Characteristics

The formation of sand wave is due to the interaction between a sandy seabed and a tidal current. Small perturbations of the sea floor can cause small perturbations in the flow filed and vice versa. Flow accelerates when the water depth decreases, which causes a slightly higher flow velocity uphill than downhill. Due to the oscillating nature of the tidal flow, if the flow field is averaged over the tidal cycle, a small vertical residual circulation cell occurs on each side of the perturbations. These cells cause small net sediment transport to the crests of the perturbations, which causes the growth of sand waves. A tidal-averaged velocity field calculated by the present model is shown in Figure 1, in which the vertical flow circulation cells distinctly exist on the both slopes of the sand wave crests and the resultant velocity along the seabed points to the crest. This is the main cause of the growth of sand waves. Then the tidal-averaged shear stress along the seabed is calculated with three different turbulence models: a constant eddy viscosity, a parabolic eddy viscosity profile in the vertical direction and a k-ε turbulence model. In Figure 2, it can be seen that the results by using a k-ε model is slightly larger than that by using a parabolic profile, and much larger than that by using a constant eddy viscosity model.

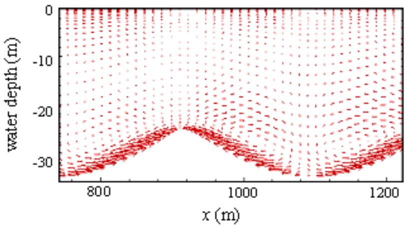

Figure 1. Tidal-average vertical flow residual circulations.

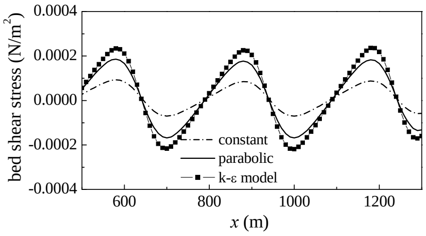

_Figure 2. Tidal-average bed shear stress with three turbulence models.

4. Sensitivity of model configuration

The sand wave simulation is usually carried out in a quite large computational area and over a very long time period. So the selection of the computational time step and the grid size is important in the numerical simulation. Here, a model sensitivity analysis is conducted on the morphological factors, the time step and the grid size in the horizontal direction to find out an optimal balance between the computational effort and the accuracy of the results.

Because the time scale for the water motion is much smaller than that for the seabed evolution, a very useful factor, namely, the morphological factor is applied in the seabed evolution to accelerate the rate of the morphological change. In programming, the bedload fluxes, erosion and deposition rates are multiplied by this scale factor after each time step.

An initial seabed with sinusoidal perturbations (2m in height and 300m in wavelength) is exposed to a tidal current to study the sensitivities of the model parameters. The depth-average velocity of the current is U=1.0m/s; period is T=12.25hr. The sand with medium size d_{50}=0.30mm is used. Water depth is 30m; the grid size in the horizontal direction is dx=10m, and time step is dt= 2.25s.

Morphological factors with value of 50, 100, 200 and 400 are examined in the analysis. The duration of each simulation is 1.1 years. Figure 3 shows the bed elevations after 1.1 year evolution with four different morphological factors. It can be seen that the morphological factor has negligible influence on the results of the sand wave evolution. So in the following simulations, a morphological factor with value of 400 is used, which improves the computational efficiency significantly.

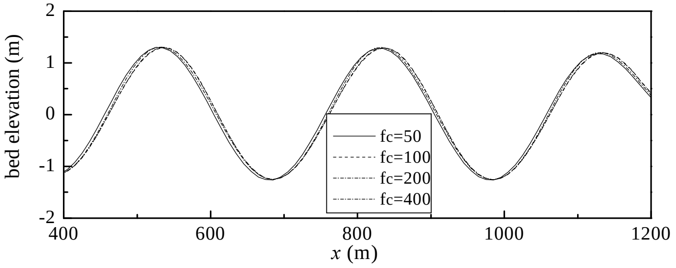

Figure 3. Evolution of sand waves after 1.1 year with different morphological factors.

Then the evolution of the same initial seabed is simulated to test the sensitivity of the time step. Four different time steps of dt= 4.5s, 3.375s, 2.25s, 1,125s are used. Figure 4 presents the bed elevations calculated with the four different time steps. The sand wave profiles converge with the decrease of the time step. The difference of the sand wave height between the case with *dt*=1.125s and that with *dt*=2.25s is less than 1%. So the time step d*t*=2.25s is used in the following simulations.

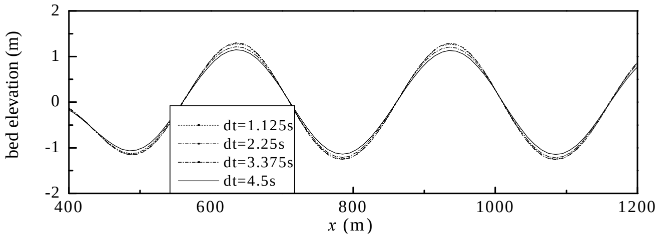

Figure 4. Evolution of sand waves after 1.1 year with different time steps.

The effect of the vertical grid level on the convergence of results has been studied in [6], and a vertical stretching grid with more than 20 levels was advised. So here, only the horizontal grid size is studied. The grid size in wavelength direction, *dx*=6m, 10m, 15m and 20m are examined. Only three results are shown in Figure 5 because the simulation with *dx*=20m did not converge. It appears that simulation results change little for *dx* values less than 10 m. Therefore *dx*=10m is used in this study.

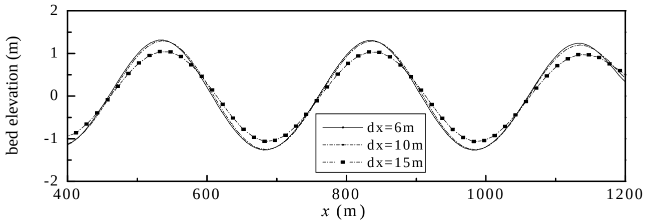

Figure 5. Evolution of sand waves after 1.1 year with different horizontal grid sizes.

5. Evolution of sand waves

5.1. *Fastest Growing Mode (FGM)*

It is commonly believed that only the Fastest Growing Mode will dominate the seabed in a very long term. FGM is the perturbation which triggers the fastest initial growth. So we can predict the wavelength of the dominant sand waves under certain circumstance by comparing their initial growth rates. For example, there is an initial seabed with perturbations in various wavelengths of 150m, 200m, 300m, 400m, 500m, 600m, 700m and 900m, exposed to an tidal current of U=1.0m/s, T=12.25hr. The sand grain size d_{50}=0.3mm is used, and the water depth is d=30m. The evolution of the initial seabed with different perturbations is simulated. Through comparing their initial growth rate, FGM can be approximately estimated, as shown in Figure 6. It can be seen that the wavelength of FGM is about 400m in both models.

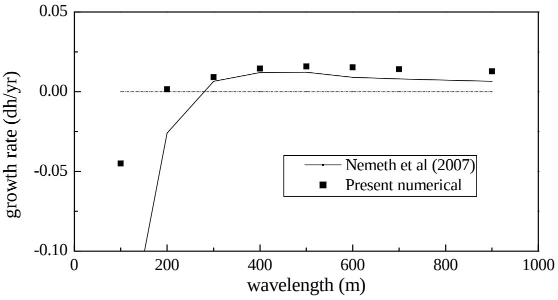

Figure 6. Growth rates for different wave length.

5.2. *Effect of parameters on FGM*

The effects of depth-average tidal flow velocity, the water depth and the sand gain size, on FGM are investigated in this study.

The evolution of sand waves with different water depth of H=12m, 20m, 30m, 40m, 60m are simulated to study its effect on FGM. The other model configurations are the same as in the case studied in the previous section. It can be seen from Figure 7 that the wave length of FGM increases with the increase of the water depth.

Then, the evolution of sand waves under five different tidal current velocities U=0.3m/s, 0.7m/s, 1.0m/s, 1.2m/s and 1.5m/s, are simulated. It can be seen from Figure 8 that the wavelength of the sand waves increases slightly with the increase of the tidal velocity.

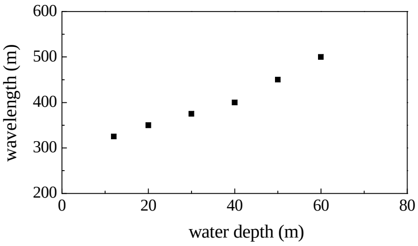

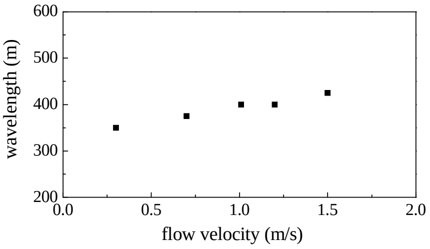

Figure 7. Wavelength of FGM vs. water depth.

Figure 8. Wavelength of FGM vs. flow velocity.

The growth rates of FGM with different sand grain sizes of d_{50}=0.1mm-1.5mm are calculated. It can be seen from Fig. 9 that the growth rate of FGM generally increases with the increase of the sand grain size, especially when d_{50}>0.5mm. When d_{50}<0.5mm, the growth rate of FGM is less dependent on the grain size. The tidal-averaged shear stress along the seabed with three different sand grain sizes is calculated further and the results are shown in Figure 10. The tidal-averaged bed shear stress increases with the increase of the grain size, which can well explain the relationship between the growth rate of FGM and the sand grain size shown in Figure 9.

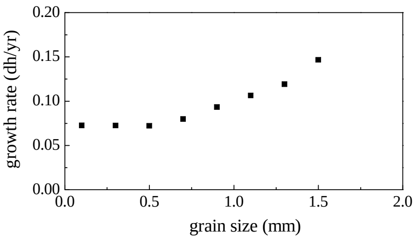

Figure 9. Growth rate vs. sand grain size.

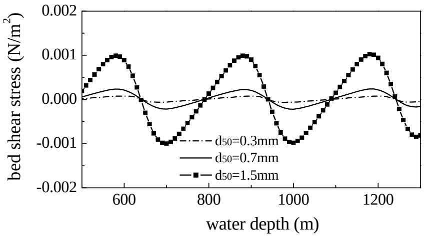

Figure 10. Tidal-mean bed shear stress along seabed with different sand grain sizes.

6. Migration of sand waves

Finally, the evolution and migration of an artificial sand wave near Hoek van Holland is simulated numerically using the present model. The sand wave was formed by dumping of the sand dredged from the shipping channel to Rotterdam since 1982. The mean tidal current is almost perpendicular to the sand wave crest and has a peak flood velocity of 0.7m/s and ebb velocity of 0.6m/s. The sand grain size is from 0.15 to 0.45mm and the water depth is from 15m-23m. The bed profiles of the artificial sand wave at three cross-sections were measured in 1986, 1991, 1995 and 2000, to investigate its evolution and migration [5].

Here, a middle segment of the sand wave was simulated to verify the present numerical model. As discussed in Nemeth et al (2002), the tidal current can be decomposed into two components: an oscillatory tidal motion and a residual current. The oscillatory component is responsible for the growth of sand waves, while the steady component is the main cause of the migration of sand waves. So in this case, the asymmetric tidal current is represented by a combination of an oscillatory current of 0.65m/s and a steady current of 0.05m/s. The bed level at 1986 is set as the initial bed. Then the evolution of sand wave is simulated for 5 years under the tidal current. Figure 11 shows the simulated 3D profiles of the sand wave in 1986 and 1991.

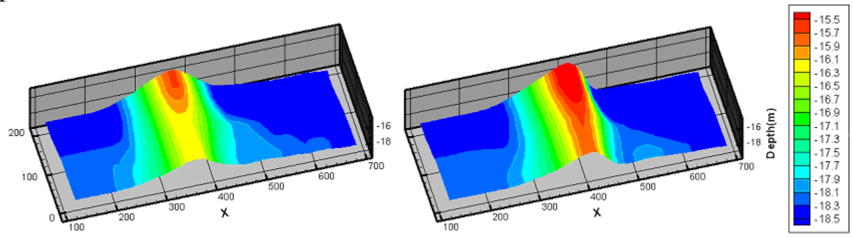

Figure11. 3-D profiles of artificial sand wave at 1986 and 1991

Figure 12 shows the comparison between numerical results and measured data for the 2-D bed elevations at cross-section 3 and cross-section 4 in 1991, and the initial bed at 1986 are also shown in figure for reference. It can be seen that the present model is able to simulate the transient behavior of sand waves and the accuracy of the model appears to be acceptable.

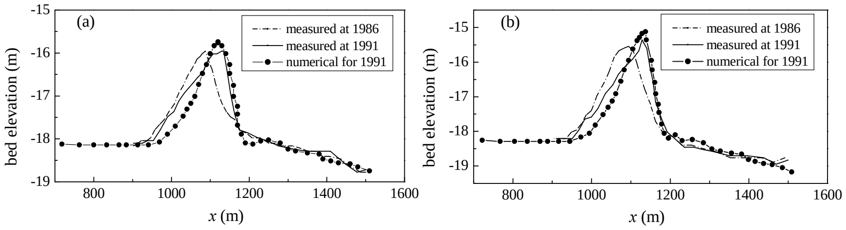

Figure12. 2-D bed elevation of artificial sand wave, (a)cross-section 3, (b)cross-section 4.

7. Discussions

In this study, a three-dimensional numerical morphdynamic sand wave model is established based on ROMS. At the current stage, the idealized cases of sand waves were simulated to test the capability of the model. A sensitivity analysis of model configurations was conducted. Then the effects of some key parameters on FGM were studied. The wavelength of FGM increases with the increase of the water depth and slightly increases with the increase of the flow velocity. The grow rate of FGM are generally increases with the increase of the sand grain size. Finally, a migrating artificial san wave under a tidal current was simulated. From the results obtained, it appears that the present model is able to simulate the transient behavior of sand waves.

Acknowledgments

This research was supported by the project “Wealth from Oceans - Subsea Pipelines for Reliable & Environmentally Safe Development of Ocean Hydrocarbon Resources - Seabed Morphology”, CSIRO Flagship Collaboration Fund Cluster, Australia.

References

1. S. J. M. H. Hulscher, *J. Geophy. Res.* **101 (C9)**, 727 (1996).
2. N. L. Komarova and S. J. M. H. Hulscher, *J. Fluid Mech.,* **413**, 219 (2000).
3. G. Besio, P. Blondeaux and G. Vittori, *J. Fluid Mech.,* **557**, 1 (2006).
4. A. A. Németh, S. J. M. H. Hulscher and R. M. J. Van Damme, *Contin. Shelf Res.,* **27**, 713 (2007).
5. P. K. Tonnon, L.C. Van Rijn and D. J. R. Walstra, *Coast. Eng.,* **54**, 279 (2007).
6. J. C. Warner, C. R. Sherwood, R. P. Signell, C. K. Harris and H. G., Arango, *Comp. Geosci.,* **34**, 1284 (2008).